Direct Access by Mechanochemistry or Sonochemistry to Protonated Merocyanines: Components of a Four-State Molecular Switch

Melwin Colaço,[b] Andrea Carletta,[a] Mégane Van Gysel,[a] Koen Robeyns,[c] Nikolay Tumanov,[a] and Johan Wouters*[a]

Direct access to the protonated merocyanine forms of two substituted spiropyrans by mechanosynthesis or sonochemistry was explored. The compounds were formed by the condensation reaction of the methyleneindolium iodide salt with salicylaldehyde derivatives. X-ray crystallography, ^{1}H NMR spectroscopy, ab initio geometry optimization, and absorption spectroscopy were combined to provide a better understanding of the four-state molecular switch system in which the newly synthesized protonated merocyanines were found to play a central role. The results of this study suggest that the stability of the protonated merocyanines requires acidic conditions, as treatment with base led to the corresponding unprotonated merocyanines, which in turn spontaneously converted into photochromic closed spiropyrans.

1. Introduction

The photochromism of spiropyrans (SPs) is well studied.[1,2] Ring-opening isomerization is triggered by UV-light irradiation and transforms a spiropyran into the corresponding planar, open merocyanine (ME) isomer (Figure 1). A colorless solution of the model molecule 1,3,3-trimethylindolino-6′-nitrobenzo-pyrylospiran (SP_NO$_2$), ($\lambda = 320$–350 nm absorption corresponding to electronic transition in the chromene moiety) turns dark purple ($\lambda = 550$–600 nm absorption corresponding to the π–π* transition in the delocalized merocyanine) upon UV-light irradiation.[3–7]

The SP⇌ME photoreaction is thermally and photochemically reversible. Among photochromic dyes, spiropyrans are a major class of reversible organic photochromes, and the merocyanine form is characterized by a high quantum yield. Thanks to their quick response times and good photo-fatigue resistance, SPs is a system-of-choice for the construction of novel dynamic materials.[2]

Detailed theoretical description of the SP⇌ME equilibrium has been reported by using quantum-mechanical calculations (DFT level) of the thermodynamic parameters for all intermediates and transition states, and the calculated activation ener-
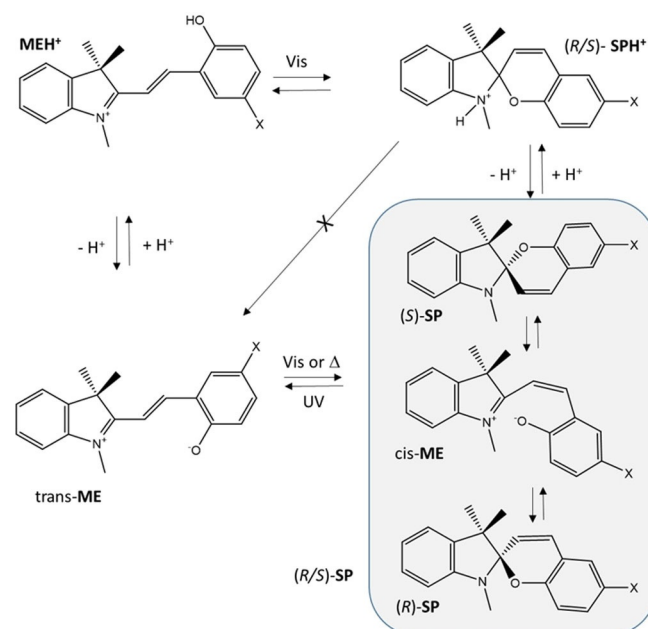
[a] A. Carletta, M. Van Gysel, N. Tumanov, Prof. J. Wouters
Department Chemistry
UNamur
61 Rue de Bruxelles, 5000 Namur (Belgium)
E-mail: johan.wouters@unamur.be

[b] M. Colaço
Department Chemistry
St. Joseph's College
Box 27094, 560 027 Bangalore (India)

[c] K. Robeyns
Department Chemistry
UCL
1 Place Louis Pasteur, 1348 Louvain-la-Neuve (Belgium)

Figure 1. Four-state molecular system involving spiropyrans. (R/S)-SP (SP from here on): spiropyran; MEH$^+$: protonated merocyanine; (R/S)-SPH$^+$ (SPH$^+$): protonated spiropyran; ME: merocyanine. Nitro-substituted compound (X=NO$_2$) has been extensively studied.[2] Compounds included in this study correspond to X=NO$_2$ and Br.

gies are reported to be in agreement with the experimental data in solution.[8,9] Depending on the nature of the substituents and the medium, the electronic distribution of ME varies from a zwitterionic form to a nonionic quinoidal structure. ME can be stabilized by highly polar solvents[10,11] and solid matrices[12–14] or through coordination to metal ions.[15–17] Encapsulation can selectively stabilize one of the isomeric forms, which enables the direct synthesis of functional and tunable solid materials.[18] Formation of salts with the protonated form (i.e., MEH$^+$) is induced in the presence of acids.[19,20]

A three-state molecular switch based on SP_NO$_2$ has been designed and investigated.[21] It combines light and chemical stimuli that transduce into optical outputs through a sequence of logic operations involving the SP, ME, and MEH$^+$ forms (Figure 1).

This three-state molecular switch detects three input signals (ultraviolet light, visible light, and H$^+$) and generates two output signals (absorption bands at $\lambda = 400$ nm for MEH$^+$ and $\lambda = 563$ nm for ME), leading to logic gates.[21,22]

Protonated ring-opened isomers of SP (protonated merocyanine form, MEH$^+$) are thermodynamically stable in acidic aqueous solutions in the dark. The effect of substituents on the spirobenzopyrans on ring opening was previously studied.[23] Substitution by an electron-withdrawing nitro group decreased the rate of ring opening, an effect that was explained by changes in the electron density of the oxygen atom of the spirobenzopyran.

Recently, the protonated open-ring merocyanine forms were obtained by recrystallization of spiropyrans in the presence of inorganic acids. In the resulting crystal structures, the counteranions (Br$^-$, Cl$^-$, SO$_4^{2-}$, and NO$_3^-$) stabilized, by formation of an hydrogen bond in the crystal packing, the primary protonated oxygen atom resulting from ring-opening isomerization.[24] The counteranions further compensated the charge of the MEH$^+$ ion.

In the present work, we directly synthesized the protonated merocyanine forms of nitro- and bromo-substituted SP (MEH$^+$, X=NO$_2$, Br) by mechano- and sonosynthesis. Mechanosynthesis consists in the use of mechanical energy to trigger chemical reactions between solids.[25–27] Solid-state reactions are therefore performed in mixer mills.[28] Among the advantages of mechanosynthesis are: large quantities of starting materials can be used, timesaving properties, and the possibility to reduce side reactions, a factor that can lead to higher yields and better conversions.[28,29] Furthermore, mechanosynthesis has been successfully employed in co-crystal synthesis[30–32] and polymorph selection,[33] allowing the generation of solid forms that are otherwise not accessible. Sonosynthesis (also called ultrasound-assisted synthesis) has been widely used in the synthesis of graphene-based materials and in the catalyst-free synthesis of a variety of organic compounds.[34,35]

The two four-state molecular switch systems (involving the two MEH$^+$ compounds) were systematically analyzed by recording UV/Vis absorption spectra in solution.

2. Results and Discussion

2.1. Synthesis

Protonated merocyanines can be transiently generated in solution upon irradiation of the corresponding spiropyrans under acidic conditions (Figure 1). Classical synthesis of the spiropyrans relies on the condensation of salicylaldehyde derivatives with 1,3,3-trimethyl-2-methyleneindoline (Fischer base). Reflux in solvents and long reaction times (2 h to 7 d) are typically required. The synthesis of spiropyrans with ultrasounds has been proposed as an interesting alternative.[36]

Recently, protonated merocyanines were directly synthesized by Knoevenagel condensation between substituted benzaldehydes and 1,2,3,3-tetramethyl-3H-indolium iodide in ethanol.[37] This procedure required long reaction times (typically 15–20 h) and was performed at a high temperature (reflux) to reach yields in the 60–85% range.

Direct access to nitro- and bromo-substituted protonated merocyanines [MEH$^+$, X=NO$_2$, Br (Figure 1)] by mechano- and sonosynthesis is reported here.

Nitro-substituted merocyanine (MEH$^+$, X=NO$_2$) was obtained by solid-state grinding of 1,2,3,3-tetramethyl-3H-indolium iodide and 5-nitrosalicylaldehyde for 90 min at 90 Hz (Scheme 1, see the Supporting Information for experimental

a = ball milling (90 mon, 30 Hz); b = recrystallization from EtOH
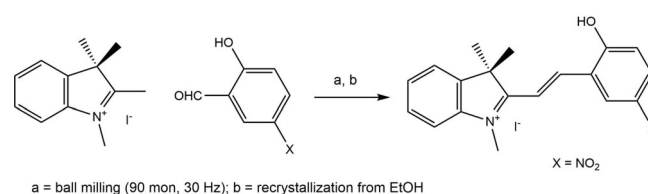
Scheme 1. Mechanosynthesis of the iodide salt of the protonated nitromerocyanine derivative.

details). Liquid-assisted grinding proved most effective with ethanol. This reaction led to the corresponding nitro-substituted merocyanine, as confirmed by powder X-ray diffraction analysis (Figure 2). Pure compound was obtained by recrystallization from ethanol. Less-reactive 4-bromosalicylaldehyde did not yield the desired product by mechanochemistry under the applied conditions.

Both protonated merocyanines (MEH$^+$, X=NO$_2$, Br) could be obtained by using sonochemistry (Scheme 2, see the Supporting Information for experimental details). Saturated solutions of the reactants (i.e., 5-nitrosalicylaldehyde or 5-bromosalicylaldehyde and 1,2,3,3-tetramethyl-3H-indolium iodide) in EtOH were placed in an ultrasound bath for 20 or 40 min, respectively, and this yielded the desired product in high yield (over 90%, as judged by ^{1}H NMR spectroscopy in [D$_6$]DMSO).

Pure crystals were obtained by slow evaporation of concentrated ethanol solutions. For each product, one proton signal was observed around $\delta = 1.8$ ppm for the two homotopic methyl groups on C3 of the indolinium ring, and this resonance confirmed formation of the open merocyanine form. In
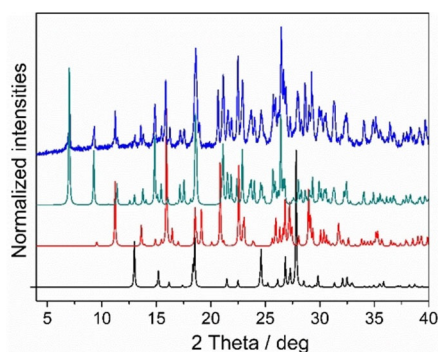
Figure 2. Powder X-ray diffractogram of the solid product obtained by liquid-assisted grinding (EtOH, ——) of 1,2,3,3-tetramethyl-3H-indolium iodide (——) and 5-nitrosalicylaldehyde (——) and comparison with the powder pattern simulated from the coordinates of protonated nitromerocyanine (MEH$^+$, X=NO$_2$, ——) determined by single-crystal X-ray crystallography.

a = sonication in EtOH; b = recrystallization from EtOH
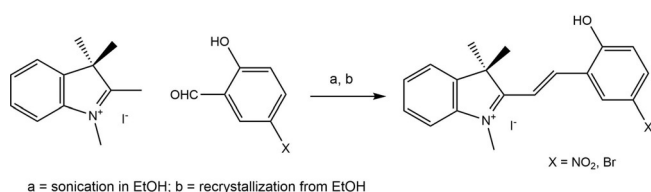
Scheme 2. Sonochemical synthesis of the iodide salts of the protonated merocyanines under study.

contrast, closed spiropyrans are characterized by two groups of proton signals observed for the two diastereotopic methyl groups,[37] a feature that was not observed as long as no base was added to the solution.

2.2. Structural Characterization

Single crystals of MEH$^+$_NO$_2$ and MEH$^+$_Br suitable for X-ray diffraction analysis were obtained by slow evaporation from saturated solutions in EtOH. Figure 3 shows the solid-state conformations of MEH$^+$_NO$_2$ and MEH$^+$_Br.

Single-crystal analysis of the compounds unequivocally established the structures of the iodide salts of the protonated merocyanines. Analysis of the bond lengths in these structures revealed conjugation that extends from the pyrrole nitrogen atom through the C=C bond to the p-nitrophenyl (MEH$^+$_NO$_2$) or bromophenyl (MEH$^+$_Br) rings. Similar electronic delocalization is observed in the zwitterionic forms associated to the ME crystal structures (e.g. CSD entry BAPNAH,[38] BETGEM[39]). The crystal structures confirm the trans-olefinic configuration and show that the protonated merocyanine cations have an almost coplanar conformation (Table 1). Indeed, the ME and MEH$^+$ conformers essentially differ by the values of the three torsion angles N1–C2–C4–C5 (α), C2–C4–C5–C6 (β), and C4–C5–C6–C7 (γ) (see Table 1 for numbering). The conformers are labeled by a three-letter code indicating the cis (C) or trans (T) value for α, β, and γ, respectively. This allows easy comparison with data from the literature adopting the same nomenclature.[8,9]
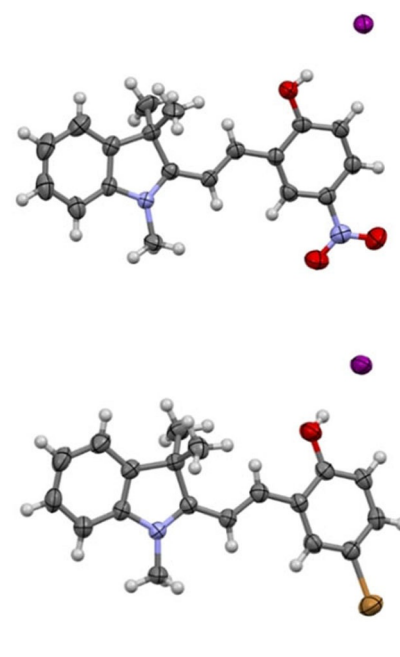

Figure 3. Crystallographic structures of the iodide salts of a) MEH$^+$_NO$_2$ and b) MEH$^+$_Br.

Table 1. Conformational analysis associated with (un)protonated merocyanines: torsion angles observed in the crystal structures of MEH$^+$_NO$_2$ and MEH$^+$_Br and the relative stabilities calculated for these systems.[a]

X-ray Crystallography					
α [°]	β [°]	γ [°]	α [°]	β [°]	γ [°]
MEH$^+$_NO$_2$			MEH$^+$_Br		
179.4(3)	179.6(3)	−168.6(4)	176.3(2)	−176.1(2)	166.7(3)

Ab Initio Calculations[b]			
Conformation[c]	ΔE [kJ mol^{-1}]		
	MEH$^+$_NO$_2$	MEH$^+$_Br	ME_NO$_2$[d]
TTT	0	1.9	4.6
TTC	0.9	0	0
CTT	5.8	7.2	9.1
CTC	6.9	6.8	7.8

[a] α: N1–C2–C4–C5, β: C2–C4–C5–C6, γ: C4–C5–C6–C7. [b] Calculated at the B3LYP/6–311g(d) level of theory. [c] TTT: α=180°, β=180°, γ=180°; TTC: α=180°, β=180°, γ=0°; CTT: α=0°, β=180°, γ=180°; CTC: α=0°, β=180°, γ=0°. [d] Taken from refs. [8,9].

In the crystal structures of both MEH$^+$_NO$_2$ and MEH$^+$_Br, the conformation corresponds to TTT. In the crystal structures, the hydroxy group of the protonated merocyanine forms a H-bond with the iodide anion [O···I 3.433(2) Å, H···I 2.61 Å, and O–H···I 178° for MEH$^+$_NO$_2$; O···I 3.433(2) Å, H···I = 2.62 Å, and O–H···I 173° for MEH$^+$_Br).

Crystal structures of protonated merocyanines are rare. One other example of such a structure is the *trans* MEH$^+$ trifluoroacetate salt of the *N*-ethanol analogue of MEH$^+$_NO$_2$ (CSD entry IHOFUG[22]).

Recently, salts of MEH$^+$_NO$_2$ were obtained by slow evaporation of a solution of SP_NO$_2$ mixed with an equimolar amount of an acid (i.e. HCl, HBr, HNO$_3$, H$_2$SO$_4$, or H$_3$PO$_4$).[25]

The crystal-structure conformations were compared to conformations obtained by ab initio energy optimizations [B3LYP/6–311g(d)]. This approach allowed us to explore the stabilities of the different possible stable conformers. Our calculations predict that TTT and TTC are favored for MEH$^+$_NO$_2$ and MEH$^+$_Br, respectively (Table 1). This is consistent with crystal structures obtained in this work, for which the TTT conformer is experimentally observed. The values computed for MEH$^+$ are also consistent with results of similar calculations performed on the MEH$^+$ and ME systems.[8, 9, 22]

2.3. Absorption Spectroscopy

The absorption properties of MEH$^+$_NO$_2$ and MEH$^+$_Br were also studied in solution in acetonitrile.

A first series of measurements were performed on the nitro-substituted molecule, as the corresponding SP_NO$_2$ derivative has been extensively studied. Figure 4 summarizes the main observations that can be made on this system. These observations are consistent with data from the literature.

The spiropyran form is usually uncolored, as this compound absorbs around $\lambda = 280$–290 nm (π–π* electronic transition in the indoline part) and $\lambda = 325$–350 nm (electronic transition of the chromene moiety). The ME form is often highly colored with absorption in the area of $\lambda = 550$ to 600 nm corresponding to the π–π* transition by the aromatic electron system delocalized through the entire molecule.[4] If a fresh solution of MEH$^+$_NO$_2$ in MeCN is passed through a plug of solid sodium carbonate, the yellow solution ($\lambda_{max} = 396$ nm) becomes dark violet ($\lambda_{max} = 558$ nm) (Figure 4a). The violet solution, associated to the unprotonated merocyanine, rapidly converts into the closed spiropyran, and this leads to a colorless solution (Figure 4b). The spiropyran converts back into the unprotonated merocyanine upon UV irradiation.

The protonated merocyanine solution is yellow and remains stable in the dark. If kept at room temperature under visible light, MEH$^+$ slowly converts into the protonated spiropyran, SPH$^+$, and this leads to a colorless solution. Deprotonation of SPH$^+$ by passing on solid Na$_2$CO$_3$ directly leads to the closed, colorless SP form.

Our approach directly gives access to the isolated protonated merocyanine form through a simple synthetic method. Indeed, to the best of our knowledge, in all previous studies this form was indirectly observed and generated, in particular through acidification of the unprotonated merocyanine obtained by UV irradiation of the closed SP form. In contrast, we produced MEH$^+$_NO$_2$ directly. Solutions of this form are stable if kept in the dark for several days.
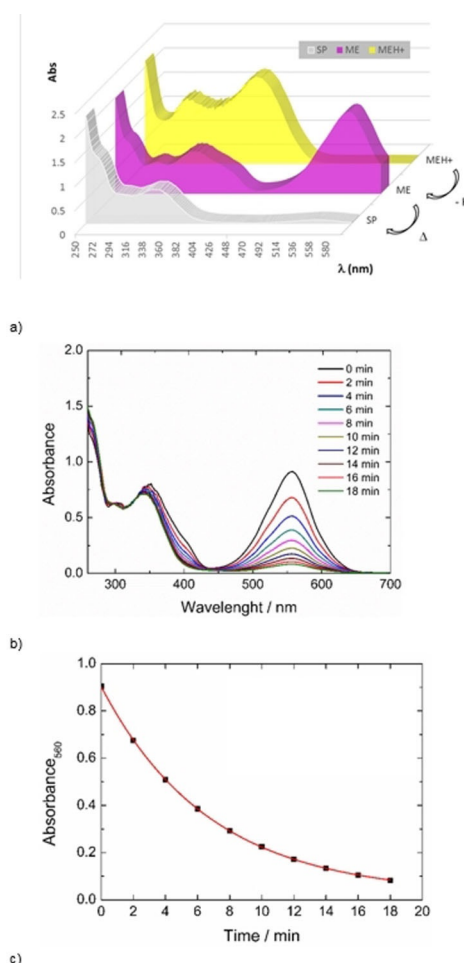

Figure 4. UV/Vis absorption spectroscopy data of MEH$^+$_NO$_2$. a) A fresh solution of the protonated merocyanine (10^{-4} M in CH$_3$CN) is yellow (MEH$^+$) and is stable if kept in the dark. It turns violet (ME) if passed through a plug of solid sodium carbonate ($-$H$^+$). b) The resulting ME form (violet solution, $\lambda_{max} = 558$ nm) returns to the stable colorless closed SP isomer within 20 min at room temperature. c) Exponential decay of SP_NO$_2$ ($t_{1/2} = 4.68 \pm 4$ min).

Figure 5a provides a general scheme for the conversions of the four-state switch starting from the protonated merocyanine form of the nitro-substituted compound, MEH$^+$_NO$_2$.

Similar analysis was performed on the bromo derivative, MEH$^+$_Br. The main results are provided in Figure 6. The overall four-state process is retained for this new compound. The protonated form obtained in our synthesis (yellow solution in MeCN, $\lambda_{max} = 431$ nm) converts into a blue solution of the unprotonated merocyanine form (ME_Br, $\lambda_{max} = 595$ nm) upon treatment with a base (sodium carbonate). The lifetime of this species is significantly shorter than that of the corresponding nitro derivative, as deduced by the evolution of the blue color over time (Figure 6c). In practice, the short-lived ME_Br form is only observable for less than 2 min at room temperature in the solvent and concentration ranges we studied. Cooling the solution extended its lifetime.

Surprisingly, the colorless solution corresponding to the closed spiropyran (SP_Br) obtained by decoloration of blue ME_Br did not revert back into the blue form upon UV light irradiation. Instead, SP_Br transformed into a new species, char-
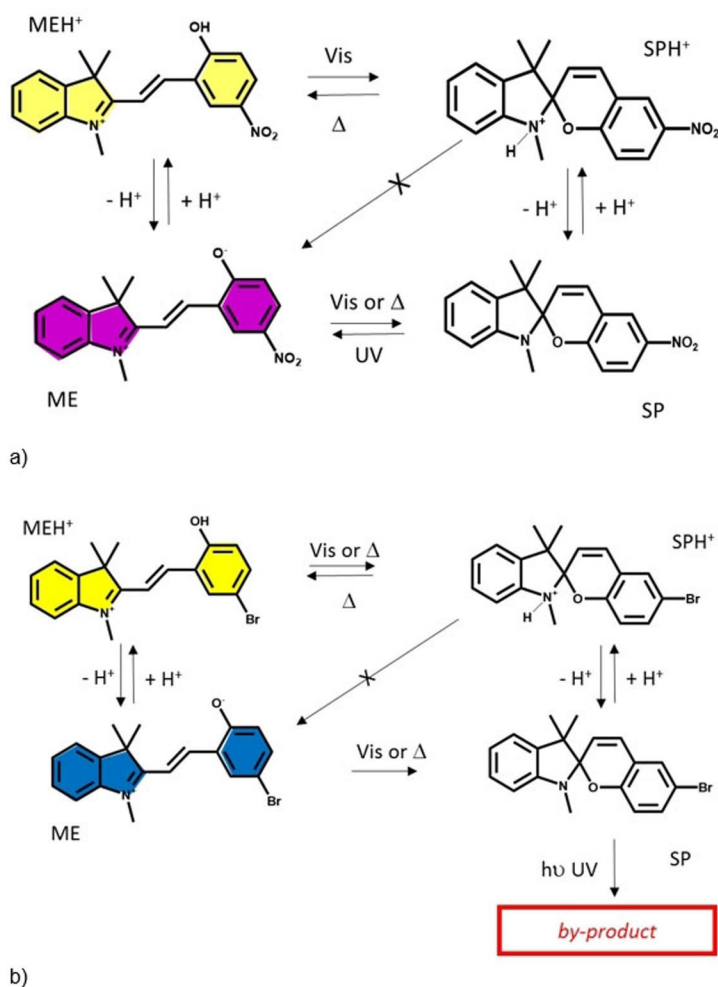
Figure 5. General schemes for the conversions of the four-state switches starting from a) MEH⁺_NO₂ and b) MEH⁺_Br.

acterized by maximum absorption at $\lambda = 475$ nm, leading to a pale-red solution (Figure 6 b). The best explanation we have so far for this observation is that upon irradiation the bromo derivative degrades into a yet to be characterized species that could result from breaking of the C—Br bond by UV irradiation, which is likely to lead to rearrangement or dimerization.

3. Conclusions

Stable solid forms of nitro- and bromo-substituted protonated merocyanines (i.e. MEH⁺_NO₂ and MEH⁺_Br) were obtained as crystalline iodide salts. The compounds were directly prepared from reactions between the corresponding salicylaldehydes and 1,2,3,3-tetramethyl-3H-indolium iodide. The more-reactive nitro-substituted compound could be obtained by mechanosynthesis. The crystal structures of both protonated merocyanines were determined and showed an all-*trans* extended open planar structure. This geometry was consistent with the computed quantum mechanics stability of the conformers. The absorption properties of MEH⁺_NO₂ and MEH⁺_Br were also studied in solution. Treatment with base led to the corresponding unprotonated merocyanines that spontaneously con-

verted into photochromic closed spiropyrans. The protonated merocyanines generated in this work are main entries to a four-state switch conversion system that could be used to design dynamic devices.

Experimental Section

Reagents were purchased from Sigma–Aldrich, TCI, and Santa Cruz BioTechnologies. Solvents were purchased from Acros Organic (Geel, Belgium) and were used without purification.

Synthesis

MEH⁺_NO₂ was synthesized by liquid-assisted grinding with a Retsch MM 400 Mixer Mill in an Eppendorf tube. Equimolar amounts of 1,2,2,3-tetramethyl-3H-indolium iodide and 5-nitrosalicylaldehyde (with two drops of ethanol) were added in a 2 mL Eppendorf tube along with seven stainless-steel grinding balls. Grinding was performed for 90 min at 30 Hz

MEH⁺_NO₂ and MEH⁺_Br were prepared by sonochemistry. Equimolar amounts of 1,2,2,3-tetramethyl-3H-indolium iodide and the substituted salicylaldehyde were placed in an Eppendorf with ethanol (0.5 mL). This tube was placed in an ultrasound bath (Bandeling Sonorex) for 20 min. This concentrated solution was evaporated.

Characterization

Single-crystal X-ray diffraction was performed with a Gemini Ultra R system (four-circle kappa platform, Ruby CCD detector) by using Mo ($\lambda = 0.71073$ Å) radiation (structure MEH⁺_NO₂) and with a Mar354 image plate (Xenocs FOX3D mirrors) by using MoKα radiation (Rotating anode RigakuUltraX 18S, Xenocs Fox3D mirrors) (structure MEH⁺_Br). Data reduction was performed by using the CrysAlisPro software package,[40] and structures were solved and refined by full-matrix least-squares refinement on IF²I (SHELXL-2014).[41]

CCDC 1833639 (MEH⁺_NO₂) and 1833640 (MEH⁺_Br) contain the supplementary crystallographic data for this paper. These data can be obtained free of charge from The Cambridge Crystallographic Data Centre.

MEH⁺_NO₂: Yellow crystals, $C_{19}H_{19}BrN_2O_3^+I^-$, triclinic, $P\bar{1}$, $a = 7.7817(4)$ Å, $b = 9.6886(6)$ Å, $c = 12.8229(8)$ Å, $\alpha = 79.940(5)°$, $\beta = 86.060(5)°$, $\gamma = 88.132(5)°$, $V = 949.43(10)$ Å³, $\rho_{calcd} = 1.575$ g cm⁻³, $F(000) = 448$, $T_{min} = 0.520$, $T_{max} = 0.907$, 4385 unique reflections, 3425 observed [$I > 2\sigma(I)$] reflections, $R1 = 0.0423$ (observed), $R1 = 0.0630$ (all), $wR2 = 0.0696$, $S = 1.084$, $\Delta\rho_{max} = 0.593$ e Å⁻³, $\Delta\rho_{min} = -0.592$ e Å⁻³.

MEH⁺_Br: Orange crystals, $C_{19}H_{19}BrNO^+I^-$, monoclinic, $P2_1/c$, $a = 9.89510(14)$ Å, $b = 12.27154(17)$ Å, $c = 15.6039(2)$ Å, $\beta = 100.9728(15)°$, $V = 1860.11(5)$ Å³, $\rho_{calcd} = 1.729$ g cm⁻³, $F(000) = 944$, $T_{min} = 0.542$, $T_{max} = 0.860$, 3443 unique reflections, 2966 observed [$I > 2\sigma(I)$] reflections, $R1 = 0.0282$ (observed), $R1 = 0.0366$ (all), $wR2 = 0.0584$, $S = 1.066$, $\Delta\rho_{max} = 0.588$ e Å⁻³, $\Delta\rho_{min} = -0.440$ e Å⁻³.

Powder X-ray diffraction (PXRD) data were collected with a PANalytical reflection-geometry diffractometer by using Ni-filtered CuKα radiation ($\lambda = 1.54179$ Å) at 40 kV and 40 mA with an X'Celerator
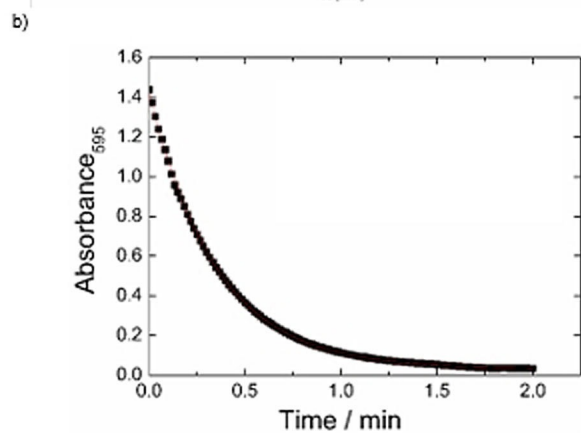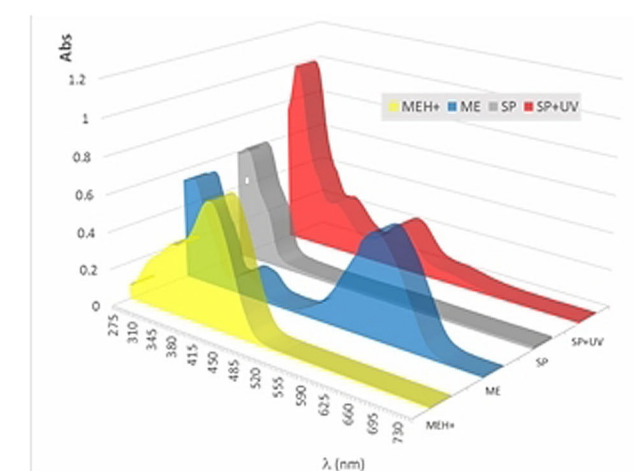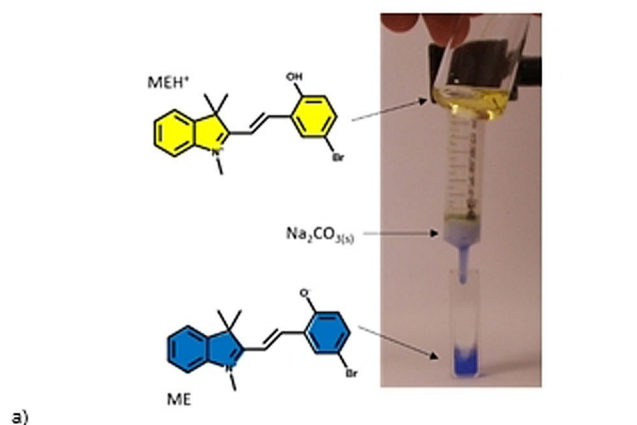
Conflict of interest

The authors declare no conflict of interest.

[1] Y. Kalisky, T. E. Orlowski, D. J. Williams, *J. Phys. Chem.* **1983**, *87*, 5333–5338.
[2] R. Klajn, *Chem. Soc. Rev.* **2014**, *43*, 148–184.
[3] J. Bonefacino, M.-L. Vincent Tse, C.-F. Jeff Pun, X. Cheng, W. Kin Edward Chan, A. Boersma, H.-Y. Tam, *Opt. Photonics J.* **2013**, *3*, 11–16.
[4] Q. Shen, Y. Cao, S. Liu, M. L. Steigerwald, X. Guo, *J. Phys. Chem. C* **2009**, *113*, 10807–10812.
[5] N. W. Tyer, R. S. Becker, *J. Am. Chem. Soc.* **1970**, *92*, 1289–1294.
[6] M. Moniruzzaman, C. J. Sabey, G. F. Fernando, *Polymer (Guildf).* **2007**, *48*, 255–263.
[7] G. Berkovic, V. Krongauz, V. Weiss, *Chem. Rev.* **2000**, *100*, 1741–1754.
[8] C. J. Wohl, D. Kuciauskas, *J. Phys. Chem. B* **2005**, *109*, 22186–22191.
[9] G. Cottone, R. Noto, G. La Manna, *Chem. Phys. Lett.* **2004**, *388*, 218–222.
[10] K. Sakai, Y. Imaizumi, T. Oguchi, H. Sakai, M. Abe, *Langmuir* **2010**, *26*, 9283–9288.
[11] J. Piard, *J. Chem. Educ.* **2014**, *91*, 2105–2111.
[12] D. Levy, *Chem. Mater.* **1997**, *9*, 2666–2670.
[13] D. Pisignano, E. Mele, L. Persano, A. Athanassiou, C. Fotakis, R. Cingolani, *J. Phys. Chem. B* **2006**, *110*, 4506–4509.
[14] B. Schaudel, C. Guermeur, C. Sanchez, K. Nakatani, J. A. Delaire, *J. Mater. Chem.* **1997**, *7*, 61–65.
[15] R. A. Kopelman, A. S. M. Snyder, N. L. Frank, *J. Am. Chem. Soc.* **2003**, *125*, 13684–13685.
[16] X. Guo, D. Zhang, A. Guanxin Zhang, D. Zhu, *J. Phys. Chem. B* **2004**, *108*, 11942–11945.
[17] M. Tanaka, M. Nakamura, M. A. Abdussalam Salhin, T. Ikeda, K. Kamada, H. Ando, Y. Shibutani, K. Kimura, *J. Org. Chem.* **2001**, *66*, 1533–1537.
[18] A. Julià-López, J. Hernando, D. Ruiz-Molina, P. González-Monje, J. Sedó, C. Roscini, *Angew. Chem. Int. Ed.* **2016**, *55*, 15044–15048; *Angew. Chem.* **2016**, *128*, 15268–15272.

Figure 6. a) Yellow-colored MEH$^+$_Br changes into the blue-colored ME form by passing through a Na$_2$CO$_3$ solid plug. b) Comparison of the UV/Vis absorption spectroscopy data of the protonated merocyanine (MEH$^+$) dissolved in solvent (10^{-4} M), merocyanine (ME) obtained by passing through a Na$_2$CO$_3$ solid plug, spiropyran (SP) obtained spontaneously by leaving ME solution in the dark, and after irradiating the SP solution (SP + UV). c) Thermal fading in the dark of the blue solution of ME showing the exponential decay in the absorption at $\lambda = 595$ nm [$t_{1/2} = (0.24 \pm 1)$ min at RT].

detector. Each sample was analyzed between $2\theta = 4$ and $50°$ with a step size of about $2\theta = 0.0167°$ and a total scan time of 3 min 48 s.

[19] A. Sugahara, N. Tanaka, A. Okazawa, N. Matsushita, N. Kojima, *Chem. Lett.* **2014**, *43*, 281–283.

[20] E. B. Gaeva, V. Pimienta, S. Delbaere, A. V. Metelitsa, N. A. Voloshin, V. I. Minkin, G. Vermeersch, J. C. Micheau, *J. Photochem. Photobiol. A* **2007**, *191*, 114–121.

[21] F. M. Raymo, S. Giordani, *J. Am. Chem. Soc.* **2001**, *123*, 4651–4652.

[22] F. M. Raymo, S. Giordani, A. J. P. White, D. J. Williams, *J. Org. Chem.* **2003**, *68*, 4158–4169.

[23] T. Satoh, K. Sumaru, T. Takagi, T. Takai, T. Kanamori, *Phys. Chem. Chem. Phys.* **2011**, *13*, 7322.

[24] V. K. Seiler, K. Callebaut, K. Robeyns, N. Tumanov, J. Wouters, B. Champagne, T. Leyssens, *CrystEngComm* **2018**, *20*, 3318–3327.

[25] F. Fischer, N. Fendel, S. Greiser, K. Rademann, F. Emmerling, *Org. Process Res. Dev.* **2017**, *21*, 655–659.

[26] A. A. L. Michalchuk, I. A. Tumanov, E. V. Boldyreva, *J. Mater. Sci.* **2018**, http://doi.org/10.1007/s10853-018-2324-2.

[27] H. Kulla, M. Wilke, F. Fischer, M. Röllig, C. Maierhofer, F. Emmerling, *Chem. Commun.* **2017**, *53*, 1664–1667.

[28] S. L. James, C. J. Adams, C. Bolm, D. Braga, P. Collier, T. Friščić, F. Grepioni, K. D. M. Harris, G. Hyett, W. Jones, A. Krebs, J. Mack, L. Maini, A. G. Orpen, I. P. Parkin, W. C. Shearouse, J. W. Steedk, D. C. Waddelli, *Chem. Soc. Rev.* **2012**, *41*, 413–47.

[29] M. Colaço, J. Dubois, J. Wouters, *CrystEngComm* **2015**, *17*, 2523–2528.

[30] A. Tilborg, G. Springuel, B. Norberg, J. Wouters, T. Leyssens, *CrystEngComm* **2013**, *15*, 3341.

[31] D. Braga, L. Maini, F. Grepioni, *Chem. Soc. Rev.* **2013**, *42*, 7638.

[32] A. Carletta, X. Buol, T. Leyssens, B. Champagne, J. Wouters, *J. Phys. Chem. C* **2016**, *120*, 10001–10008.

[33] A. Carletta, F. Spinelli, S. d'Agostino, B. Ventura, M. R. Chierotti, R. Gobetto, J. Wouters, F. Grepioni, *Chem. Eur. J.* **2017**, *23*, 5317–5329.

[34] K. Muthoosamy, S. Manickam, *Ultrason. Sonochem.* **2017**, *39*, 478–493.

[35] B. Banerjee, *Ultrason. Sonochem.* **2017**, *35*, 1–14.

[36] T. R. Silvia, V. S. L. Ana, E. A. S. González, *Synth. Commun.* **1995**, *25*, 105–110.

[37] A. Promchat, P. Rashatasakhon, M. Sukwattanasinitt, *J. Hazard. Mater.* **2017**, *329*, 255–261.

[38] J. Hobley, V. Malatesta, R. Millini, L. Montanari, W. O Neil Parker Jr, *Phys. Chem. Chem. Phys.* **1999**, *1*, 3259–3267.

[39] S. M. Aldoshin, L. O. Atovmyan, O. A. D'yachenko, M. A. Gal'bershtam, *Bull. Acad. Sci. USSR Div. Chem. Sci. (Engl. Transl.)* **1981**, *30*, 2262–2270.

[40] Rigaku Oxford Diffraction, CrysAlisPro Software System, Oxford, UK, **2015**.

[41] G. M. Sheldrick, *Acta Crystallogr.* **2015**, *C71*, 3–8.